Impact of the metal electrode size in half-cells studies: example of graphite/Li coin cells

Lénaïc Madec[a,b,*] and Hervé Martinez[a,b]

[a] *Université de Pau et des Pays de l'Adour / CNRS UMR 5254, IPREM, 2 Av. Pierre Angot, 64053 Pau, France*
[b] *Réseau sur le Stockage Electrochimique de l'Energie (RS2E), CNRS FR3459, 33 Rue Saint Leu, 80039 Amiens Cedex, France*

Corresponding authors: lenaic.madec@univ-pau.fr

Graphical abstract

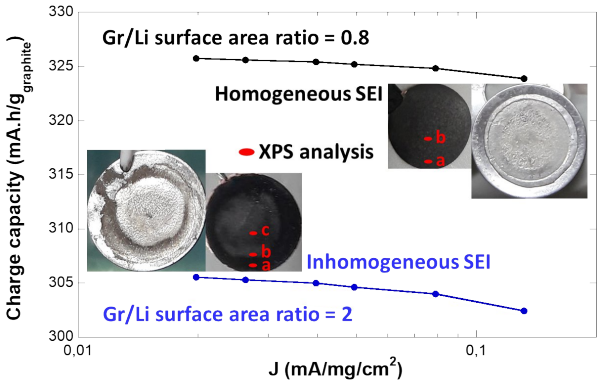

Abstract

When half-cells are used to evaluate and understand electrochemical performance and interface properties of a given electrode, the metal electrode size is rarely mentioned. To evaluate such impact on the electrochemical performance and interphase formation, graphite/Li coin cells were used. Undersizing the Li metal electrode led to significantly lower charge/discharge capacities even at C/20 rate due to incomplete lithiation/delithiation processes of the graphite electrode edge. It also led to the formation of non-uniform Li metal deposits as well as to a graphite SEI film with a thickness and composition gradient across the electrode. Oversized Li led, however to homogeneous graphite SEI film. Overall, these results highlight the critical role of the metal electrode size in half-cells and should apply to all half-cells studies using other metal electrodes such as Na, K, Mg.

Introduction

Since the introduction of the solid electrolyte interphase (SEI)[1] model to describe the surface films that forms at the electrode/electrolyte interfaces by degradation of electrolyte

solvents and/or salts under cycling/storage of Li-ion cells, numerous studies have been reported.[2],[3],[4],[5] Most of these studies use, however, half-cells with Li metal as the counter electrode, which is unlikely to depict full-cells for various aspects. First, the Li metal is likely to act as an infinite source of Li. Second, the high reactivity of the lithium metal against the electrolyte is likely to produce more and/or different electrolyte degradation species that have a high probability to migrate to the studied electrode surface then interact. Such phenomenon is called interactions between electrodes or cross-talk,[6],[7],[8] the most known being the dissolution of positive active materials at high voltage and the deposition of metal-based species at the negative electrodes surface.[9] This topic still suffer, however, a lack of attention despite recent dedicated studies.[10],[11],[12],[13],[14],[15] As a whole, in half-cells, the use of a theoretical infinite source of Li and the interactions between electrodes can greatly alter the electrochemical performance and the interphase of the studied electrode. Therefore, the half-cells should be preferably restricted to electrochemical mechanism studies of new material rather than used to extrapolate and predict the full-cells behaviour. Moreover, despite the plethora of half-cells studies, the Li metal electrode size (i.e. the surface area) is almost never mentioned probably because it is considered as an infinite source of Li. This means that, the Li metal electrode surface area may be either oversized or undersized compared to the studied electrode.

Here, as the Li metal surface area may be crucial to both the electrochemical performance and interphase formation, this impact was investigated in the case of graphite/Li cells.

2. Experimental

2.1 Cell preparation and cycling protocol

The electrolyte was 1 M $LiPF_6$ (battery grade, purity ≥99.99%) in EC(anhydrous, 99% purity):EMC(purity ≥98%) with a 3:7 weight ratio (water content <50 ppm), from Aldrich. Graphite electrode, made of artificial graphite:CMC+SBR:carbon black with a 95.7:2.9:1.4 weight ratio (6.15 $mg_{graphite}/cm^2$, 60 ± 2 µm thick after calendaring), coated on a copper foil (9 µm thick), were obtained from S4R (Castelnau-le-Lez, France). Graphite electrodes were heated at 80°C under vacuum for 12 h. Graphite/Li 2032 coin cells were assembled under Ar with 0.11 ml of electrolyte and two PPP separators. Note that varying the electrolyte amount is more likely an important parameter when studying the interphase formation but have been kept constant and in excess (due to the coin cell mounting) in the present case. The graphite/Li surface area ratio was set to 0.95 cm^2 / 1.13 cm^2 = 0.84 (Gr/Li-0.8 cells) and 1.27

cm^2 / 0.64 cm^2 = 1.98 (Gr/Li-2 cells). The latter (i.e. 1.98 ratio) was selected so that if significant changes have occurred, they could have been observed visually and they could have been characterized by XPS at different positions along the oversized graphite region considering an elliptic X-ray beam spot of about 450 x 900 µm.

Using a MPG battery cycler (Biologic SA, France), cells were held at OCV during 30 min for wetting completion then cycled between 0.005-1.2 V at C/20 for two cycles. Cells were discharged to 0.005 V at C/20 followed by a potential hold at 0.005 V until a C/100 current was reached. A power test was performed by successive charge current pulses of C/3, C/5, C/8, C/10, C/15, C/20 with a 1h OCV relaxation between each pulse. A final cycle was performed between 0.005-1.2 V at C/20. All currents refer to 372 $mAh/g_{graphite,}$ i.e. all currents were set according to the individual graphite electrode mass so that a given current in mAh/cm^2 was strictly identical whatever the electrode was.

Coin cells were then opened under argon and graphite electrodes were washed twice by immersion in a glass vial containing 0.8 ml of EMC during 10 s.

2.2 X-ray Photoelectron Spectroscopy (XPS)

XPS was performed using an Escalab 250 Xi spectrometer using a monochromatized Al Kα radiation (hν =1486.6 eV). Electrode samples were put on a sample holder using an insulating uPVC tape (reference 655 from 3M) then the samples transfer was performed through an argon-filled glove box directly connected to the spectrometer. Before analysis, samples were kept at 10^{-8} mbar for one night. Analysis was performed using the standard charge compensation mode and an elliptic 450 x 900 µm X-ray beam spot. Core spectra were recorded using a 20 eV constant pass energy with a 0.15 eV step size and short time iterative scans. Using CasaXPS software, the binding energy scale was calibrated from the 285 eV peak (C-C/C-H). A non-linear Shirley-type background was used for core peaks analysis while 70% Gaussian - 30% Lorentzian Voigt peak shapes and full width at half-maximum constraint ranges were selected to optimize areas and peak positions. XPS quantification were performed using the relative sensitivity factor provided with the Escalab machine.

3. Results

3.1 Electrochemical performance

Figure 1 shows a) the potential versus time curves and b) the charge capacity versus the specific current J ($mA/mg/cm^2$) for Gr/Li-0.8 and Gr/Li-2 cells. Both cells showed very close shape of the discharge/charge curves with the reversible lithiation stages of the graphite.[16]

Gr/Li-2 cells showed, however, shorter discharge/charge time compared to Gr/Li-0.8 cells (Figure 1a) due to lower capacities (Figure 1b). Indeed, Gr/Li-2 cells delivered about 5.5% lower charge capacity (corresponding to 18 mA.h/$g_{graphite}$) compared to Gr/Li-0.8 cells even at a very slow rate (C/20). This result is explained by incomplete lithiation/delithiation processes of the graphite electrode edge due to the Li metal electrode undersizing and despite that Li metal is considered as an infinite Li source.

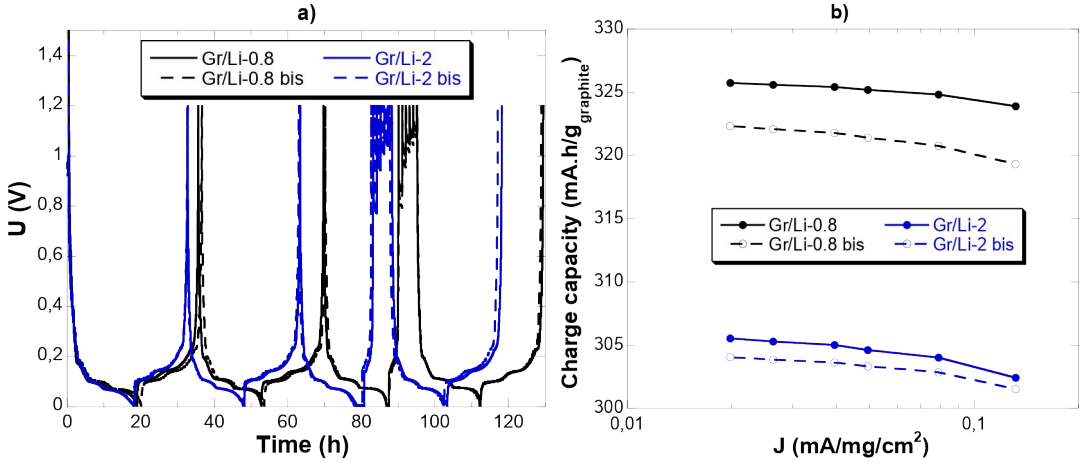

Figure 1. a) Potential versus time curves and b) charge capacity (mAh/$g_{graphite}$) versus the specific current J (mA/mg/cm^2) for the Gr/Li-2 and Gr/Li-0.8 cells. The notation ‘’bis’’ stands for the second pair cell.

3.2 Cells disassembly

Figure 2 shows the photographs of cycled lithium and graphite electrodes as extracted from the a) Gr/Li-0.8 and b) Gr/Li-2 cells with respect to the real scale. When oversizing the Li metal electrode (Gr/Li-0.8 cells), relatively uniform Li and graphite electrodes were observed (Figure 2a). Note that the superimpose region of the Li metal electrode (relative to the graphite) appeared slightly more grey than the oversized region due to the SEI film formation. Note also that no Li plating deposit was observed around the graphite electrode (not shown) more likely due to the relatively low cycling rate used in the present case. Undersizing the Li led (Gr/Li-2 cells), however, to non-uniform Li and graphite electrodes with two distinct regions (Figure 2b). The Li metal showed a grey color due to the SEI film formation and were surrounded by non-uniform Li plating deposits. Similarly, the graphite regions superimpose to the Li, showed a different color than the oversized graphite regions. These phenomena are explained by the partial lithiation/delithiation of the graphite electrode edge due to the Li metal undersizing. Moreover, the appearance of two distinct regions on the graphite electrodes suggests the formation of different SEI films.

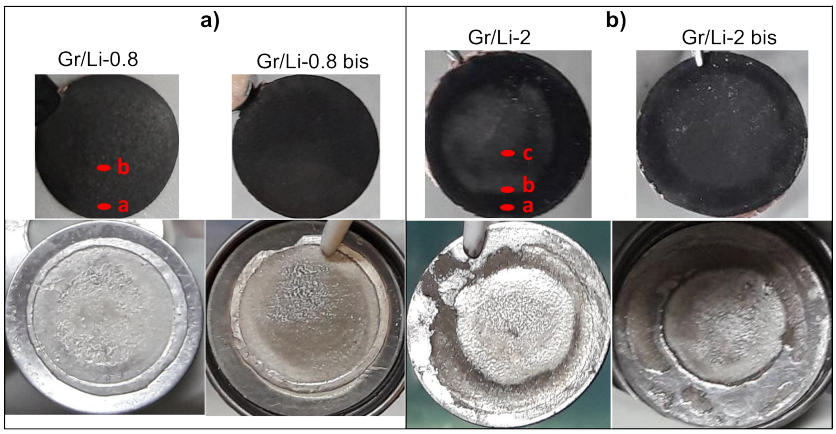

Figure 2. Photographs of the lithium and graphite electrodes as extracted from the a) Gr/Li-0.8 and b) Gr/Li-2 cells with respect to the real scale. Red spots indicate area where XPS analysis were performed.

3.3 XPS analysis of the graphite electrodes

To evaluate the graphite SEI films homogeneity for both Gr/Li-0.8 and Gr/Li-2 cells, XPS analysis was performed at different position as indicated by the red spot in Figure 2. The corresponding a) carbon 1s and b) oxygen 1s XPS core spectra are showed in Figure 3. Note that both graphite pair electrodes as well as additional positions were also analyzed for reproducibility but are not showed here for clarity and brevity. In Figure 3, the core level spectra for a given element were normalized to show the relative intensity/amount of the given element between samples.[14],[17]

The C 1s spectrum of fresh graphite electrode showed five components at 284.1 (C=C), 286.9 (CO), 288.7 (CO_2), 291.2 eV (‘’shake up’’ satellite) from the graphite and 285.0 eV (C-C/C-H) from the SBR binder[18] and graphite[19]·[20] (Figure 3a). The O 1s spectrum of the fresh graphite electrode showed two peaks at 531.8 and 533.5 eV from the CMC binder (Figure 3b).[18] An additional peak was also observed at 536.5 eV due to Na Auger from the CMC binder (Figure 3b).[21] After cycling, two C=C peaks from the graphite were observed at ~283.5 eV and ~282.4 eV, probably due to a differential charging effect.[22] After cycling, the overall intensity of these graphite peaks decreased due to the partial covering of the graphite by SEI films. This phenomenon was, however, more pronounced for Gr/Li-0.8 indicating the formation of thicker SEI films compared to Gr/Li-2. Interestingly, no significant C=C peaks evolution was observed for Gr/Li-0.8 between the edge and the center of the electrode indicating the formation of a homogeneous SEI film at the graphite surface. At the opposite, Gr/Li-2 showed increasing intensities of the C=C peaks from the edge to the center of the electrode indicating the formation of a SEI with a thickness gradient across the electrode due to the Li metal undersizing.

After cycling, the two main O 1s peaks of the fresh graphite were replaced by new components (Figure 3b), in agreement with the formation of carbonaceous species from the solvents at the graphite and CMC surfaces. The peak at 533.4 eV is attributed to CO bonds mainly from ether derivatives and low amounts of $ROCO_2Li$ [23],[24] while the peak at 530.5 eV is assigned to lithium alkoxide (ROLi)[14],[25] in agreement with the corresponding at.% of these peaks and the at.% of the CO carbon 1s peak (Figure 3a). The peak at 531.7 eV is attributed mainly to Li_2CO_3, RCO_2Li and PO_x compounds as well as low amounts of $ROCO_2Li$ species[26],[27] while the peak at 528.5 eV is due to the formation of lithium oxide (Li_2O).[28],[29] The corresponding carbon 1s peaks for Li_2CO_3 and RCO_2Li were observed at 290.1 eV and 289.0 eV, respectively. Additionally, LiF was found in the SEI with the presence of a fluorine 1s peak at 685.1 eV (not shown). The corresponding LiF at.% are reported on Figure 3a. As a whole, no significant change of composition was observed for Gr/Li0.8 between the edge and the center of the electrode, which indicates the formation of a homogeneous SEI film. At the opposite, Gr/Li-2 showed increasing amounts of Li_2CO_3 (290.1 eV), RCO_2Li (289.0 eV) and decreasing amounts of ROLi (530.5 eV), ether derivatives (533.4 eV) and LiF from the edge to the center of the electrode. This result means that undersizing the Li metal (Gr/Li-2) leads to the formation of a SEI with a composition gradient across the electrode.

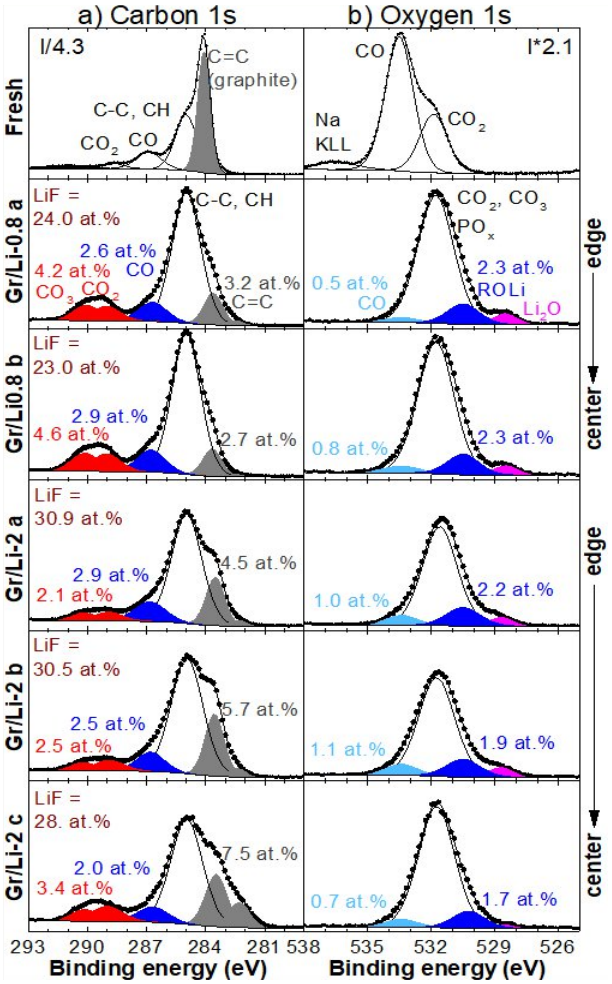

Figure 3. XPS core spectra of a) carbon 1s and b) oxygen 1s of the graphite electrodes as extracted from the Gr/Li-0.8 and Gr/Li-2 cells after cycling. Red spots in Figure 2 indicate the different positions of the electrode where the XPS analysis were performed. Typical spectra of the fresh graphite electrode are presented for comparison. Atomic Percentage (at. %) of indicated species as obtained from the XPS quantification are presented for better clarity.

Conclusion

In this paper, the impact of the metal surface area on the electrochemical performance and interphase formation in half-cells was investigated using graphite/Li coin cells. For undersized Li metal electrode, significantly lower charge/discharge capacities were observed even at very slow cycling rate due to incomplete lithiation/delithiation processes of the graphite electrode edge. Moreover, XPS analysis showed the formation of a SEI film with a thickness and composition gradient across the electrode. At the opposite, higher capacities and a very homogeneous SEI film was observed using oversized Li metal electrode. Overall, these results highlight the critical impact of the Li metal electrode size in half-cells studies if one wants to obtain reliable results. More generally, this should also apply to half-cells studies using other metal electrodes such as Na, K, Mg. Therefore, it raises the relevance of using

half-cells to investigate electrochemical performance and interphase formation in Li-ion batteries and beyond.

References

[1] E. Peled, the Electrochemical-Behavior of Alkali and Alkaline-Earth Metals in Non-Aqueous Battery Systems - the Solid Electrolyte Interphase Model, J. Electrochem. Soc. 126 (1979) 2047–2051. doi:10.1149/1.2128859.

[2] K. Xu, Electrolytes and interphases in Li-ion batteries and beyond, Chem. Rev. 114 (2014) 11503–11618. doi:10.1021/cr500003w.

[3] T. Waldmann, A. Iturrondobeitia, M. Kasper, N. Ghanbari, F. Aguesse, E. Bekaert, L. Daniel, S. Genies, I.J. Gordon, M.W. Löble, E. De Vito, M. Wohlfahrt-Mehrens, Review—Post-Mortem Analysis of Aged Lithium-Ion Batteries: Disassembly Methodology and Physico-Chemical Analysis Techniques, J. Electrochem. Soc. 163 (2016) A2149–A2164. doi:10.1149/2.1211609jes.

[4] S.J. An, J. Li, C. Daniel, D. Mohanty, S. Nagpure, D.L. Wood, The state of understanding of the lithium-ion-battery graphite solid electrolyte interphase (SEI) and its relationship to formation cycling, Carbon N. Y. 105 (2016) 52–76. doi:10.1016/j.carbon.2016.04.008.

[5] K. Kleiner, H. Ehrenberg, Challenges Considering the Degradation of Cell Components in Commercial Lithium-Ion Cells: A Review and Evaluation of Present Systems, Top. Curr. Chem. 375 (2017) 1–45. doi:10.1007/s41061-017-0139-2.

[6] S.E. Sloop, J.B. Kerr, K. Kinoshita, The role of Li-ion battery electrolyte reactivity in performance decline and self-discharge, J. Power Sources. 119–121 (2003) 330–337. doi:10.1016/S0378-7753(03)00149-6.

[7] R. Dedryvère, D. Foix, S. Franger, S. Patoux, L. Daniel, D. Gonbeau, Electrode/Electrolyte Interface Reactivity in High-Voltage Spinel LiMn 1.6 Ni 0.4 O 4 /Li 4 Ti 5 O 12 Lithium-Ion Battery, J. Phys. Chem. C. 114 (2010) 10999–11008. doi:10.1021/jp1026509.

[8] J.C. Burns, A. Kassam, N.N. Sinha, L.E. Downie, L. Solnickova, B.M. Way, J.R. Dahn, Predicting and Extending the Lifetime of Li-Ion Batteries, J. Electrochem. Soc. 160 (2013) A1451–A1456. doi:10.1149/2.060309jes.

[9] Y. Talyosef, B. Markovsky, G. Salitra, D. Aurbach, H. Kim, S. Choi, The study of LiNi0.5Mn1.5O4 5-V cathodes for Li-ion batteries, J. Power Sources. 146 (2005) 664–669. doi:10.1016/j.jpowsour.2005.03.064.

[10] M. Metzger, B. Strehle, S. Solchenbach, H.A. Gasteiger, Origin of H 2 Evolution in LIBs: H 2 O Reduction vs. Electrolyte Oxidation, J. Electrochem. Soc. 163 (2016) A798–A809. doi:10.1149/2.1151605jes.

[11] R. Petibon, L. Madec, L.M. Rotermund, J.R. Dahn, Study of the consumption of the additive prop-1-ene-1,3-sultone in Li[Ni0.33Mn0.33Co0.33]O2/graphite pouch cells and evidence of positive-negative electrode interaction, J. Power Sources. 313 (2016) 152–163. doi:10.1016/j.jpowsour.2016.02.054.

[12] D.J. Xiong, R. Petibon, M. Nie, L. Ma, J. Xia, J.R. Dahn, Interactions between Positive and Negative Electrodes in Li-Ion Cells Operated at High Temperature and High Voltage, J. Electrochem. Soc. 163 (2016) A546–A551. doi:10.1149/2.0951603jes.

[13] D.J. Xiong, L.D. Ellis, R. Petibon, T. Hynes, Q.Q. Liu, J.R. Dahn, Studies of Gas Generation , Gas Consumption and Impedance Growth in Li-Ion Cells with Carbonate or Fluorinated Electrolytes Using the Pouch Bag Method, 164 (2017) 1–9. doi:10.1149/2.1091702jes.

[14] L. Madec, L.D. Ellis, Exploring Interactions between Electrodes in Li[NixMnyCo1-xy]O2/Graphite Cells through Electrode/Electrolyte Interfaces Analysis, J. Electrochem. Soc. 164 (2017) A3718–A3726. doi:10.1149/2.1011714jes.

[15] L.D. Ellis, J.P. Allen, L.M. Thompson, J.E. Harlow, W.J. Stone, I.G. Hill, J.R. Dahn, Quantifying, Understanding and Evaluating the Effects of Gas Consumption in Lithium-Ion Cells, J. Electrochem. Soc. 164 (2017) A3518–A3528. doi:10.1149/2.0191714jes.

[16] J.R. Dahn, Phase diagram of LixC6, Phys. Rev. B. 44 (1991) 9170–9177.

[17] L. Madec, L. Ma, K.J. Nelson, R. Petibon, J.-P. Sun, I.G. Hill, J.R. Dahn, The Effects of a Ternary Electrolyte Additive System on the Electrode/Electrolyte Interfaces in High Voltage Li-Ion Cells, J. Electrochem. Soc. 163 (2016) A1001–A1009. doi:10.1149/2.1051606jes.

[18] L. El Ouatani, R. Dedryvère, C. Siret, P. Biensan, S. Reynaud, P. Iratçabal, D. Gonbeau, The Effect of Vinylene Carbonate Additive on Surface Film Formation on Both Electrodes in Li-Ion Batteries, J. Electrochem. Soc. 156 (2009) A103–A113. doi:10.1149/1.3029674.

[19] D. Pantea, H. Darmstadt, S. Kaliaguine, L. Sümmchen, C. Roy, Electrical conductivity of thermal carbon blacks, Carbon N. Y. 39 (2001) 1147–1158. doi:10.1016/S0008-6223(00)00239-6.

[20] D. Pantea, H. Darmstadt, S. Kaliaguine, C. Roy, Electrical conductivity of conductive

carbon blacks: influence of surface chemistry and topology, Appl. Surf. Sci. 217 (2003) 181–193. doi:10.1016/S0169-4332(03)00550-6.

[21] A. Darwiche, L. Bodenes, L. Madec, L. Monconduit, H. Martinez, Impact of the salts and solvents on the SEI formation in Sb/Na batteries: An XPS analysis, Electrochim. Acta. 207 (2016) 284–292. doi:10.1016/j.electacta.2016.03.089.

[22] K. Ciosek Högström, S. Malmgren, M. Hahlin, M. Gorgoi, L. Nyholm, H. Rensmo, K. Edström, The buried carbon/solid electrolyte interphase in li-ion batteries studied by hard x-ray photoelectron spectroscopy, Electrochim. Acta. 138 (2014) 430–436. doi:10.1016/j.electacta.2014.06.129.

[23] R. Dedryvère, L. Gireaud, S. Grugeon, S. Laruelle, J.M. Tarascon, D. Gonbeau, Characterization of lithium alkyl carbonates by X-ray photoelectron spectroscopy: Experimental and theoretical study, J. Phys. Chem. B. 109 (2005) 15868–15875. doi:10.1021/jp051626k.

[24] S. Malmgren, K. Ciosek, M. Hahlin, T. Gustafsson, M. Gorgoi, H. Rensmo, K. Edström, Comparing anode and cathode electrode/electrolyte interface composition and morphology using soft and hard X-ray photoelectron spectroscopy, Electrochim. Acta. 97 (2013) 23–32. doi:10.1016/j.electacta.2013.03.010.

[25] M. Onuki, S. Kinoshita, Y. Sakata, M. Yanagidate, Y. Otake, M. Ue, M. Deguchi, Identification of the Source of Evolved Gas in Li-Ion Batteries Using #2#1 -labeled Solvents, J. Electrochem. Soc. 155 (2008) A794–A797. doi:10.1149/1.2969947.

[26] D. Aurbach, Identification of Surface Films Formed on Lithium in Propylene Carbonate Solutions, J. Electrochem. Soc. 134 (1987) 1611–1620. doi:10.1149/1.2100722.

[27] M. Nie, D.P. Abraham, Y. Chen, A. Bose, B.L. Lucht, Silicon Solid Electrolyte Interphase (SEI) of Lithium Ion Battery Characterized by Microscopy and Spectroscopy Silicon solid electrolyte interphase (SEI) of lithium ion battery characterized by microscopy and spectroscopy, J. Phys. Chem. C. 117 (2013) 1257–1267. doi:10.1021/jp404155y.

[28] I. Ismail, A. Noda, A. Nishimoto, M. Watanabe, XPS study of lithium surface after contact with lithium-salt doped polymer electrolytes, Electrochim. Acta. 46 (2001) 1595–1603. doi:10.1016/S0013-4686(00)00758-1.

[29] L.J. Rendek, G.S. Chottiner, D.A. Scherson, The Reactivity of Linear Alkyl Carbonates toward Metallic Lithium X-Ray Photoelectron Spectroscopy Studies in Ultrahigh Vacuum, J. Electrochem. Soc. 149 (2002) E408–E412. doi:10.1149/1.1507595.